

## Cardiac Tagging with Breath-Hold Cine MRI

ELLIOT R. McVEIGH AND ERGIN ATALAR \*

*Departments of Biomedical Engineering and Radiology, Johns Hopkins University School of Medicine, Baltimore, Maryland 21205; and \* Department of Electrical and Electronics Engineering, Bilkent University, Ankara, Turkey 06533*

Received July 14, 1992; revised September 14, 1992; accepted October 5, 1992

A method is presented for measuring myocardial deformation in a breath-hold with tagged cine MRI. Tagged cine images of human hearts are obtained in arbitrary oblique planes on a standard imager with as few as four heartbeats. The scan time has been reduced 16- to 64-fold from previous techniques. © 1992 Academic Press, Inc.

### INTRODUCTION

Over the past 4 years, a number of techniques have been developed for measuring the patterns of myocardial strain with MRI (1-5). It is possible to measure the position of presaturation tags to within 0.1 mm giving us the potential to measure myocardial strain with very high accuracy and precision (4-6). However, the quality of the underlying spin-echo cardiac images has been inconsistent due to the motion of the heart during patient breathing and the reliance on a series of 256 identical heartbeats per image acquisition. Figure 1 demonstrates a 1-cm excursion of the heart in the chest from inspiration to expiration during normal breathing. Two things are clear from this figure. Unless data acquisition is performed in a breath-hold (i) one cannot claim to measure positions in the heart consistently with an accuracy on the order of millimeters and (ii) severe blurring and ghosting will be generated from respiratory motion. In this paper we demonstrate the use of gradient-recalled acquisition in the steady state (GRASS) coupled with electrocardiogram (ECG)-gated segmented *k*-space acquisition (7) to produce movie sequences of the heart with 24 ms time resolution in 4-16 heartbeats. The limited extent of the Fourier coefficients of a parallel line tagging pattern is used to reduce the data acquisition time for heart wall motion measurements.

### MATERIALS AND METHODS

#### *Hardware*

The pulse sequence was designed for a standard Signa 4.7 MRI scanner (General Electric Medical System, Milwaukee, WI). The important performance features to note for this work are the nominal slew rate of 2 Gauss/cm/s and a maximum amplitude of 1 Gauss/cm for the self-shielded gradients. The allowable duty cycle for the amplifiers and coils is 44% at full amplitude. This does not present a limitation for the sequence described here. A  $\pm 32$ -kHz bandwidth filter was available, and a standard surface coil was used.

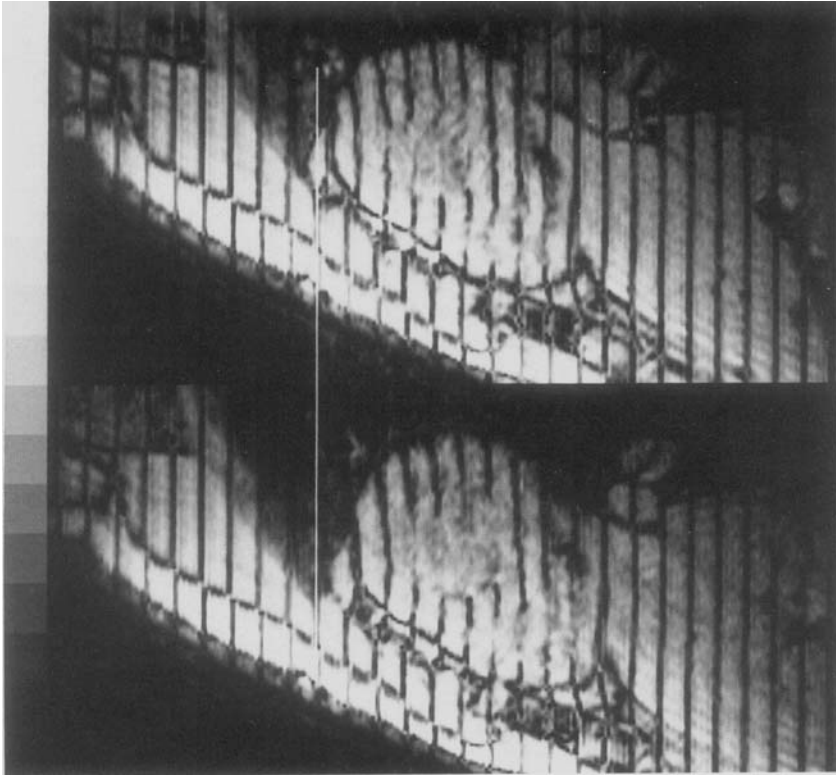


FIG. 1. Two end-diastolic coronal images of the heart at (top) inspiration and (bottom) expiration with normal breathing amplitude. These images were obtained in 16 heartbeats with breathing suspended. The heart has translated approximately 1 cm from (top) to (bottom) due only to differences in lung inflation.

### *Imaging Pulse Sequence*

The segmented  $k$ -space pulse sequence is shown in Fig. 2. Figure 2a shows the timing diagram of the GRASS sequence used to sample lines of  $k$ -space. The TR and TE are minimized by using maximum slew rate ramps and maximum amplitude constants for all gradient waveforms. The rf pulse duration is reduced for a given slice thickness by using a maximum amplitude slice selection gradient; because low flip angles are used when imaging, the rf pulses can have a short duration. Therewinder pulse of the phase encoding gradient overlaps the ascending portion of the slice selection gradient for the next excitation. The flip angle is set to  $20^\circ$  which was determined to be optimal by experiment; however, the signal-to-noise maximum is very broad with respect to flip angle. While spoiled-GRASS (8) does not require a rewinder pulse and therefore can achieve a shorter TR, we chose to use GRASS because simulations predicted better signal-to-noise and contrast characteristics; experiments must be performed to verify these predictions.

The Fourier space of the image is sampled with the segmented  $k$ -space approach as described by Atkinson and Edelman (7). Figure 2b shows the sequence of phase

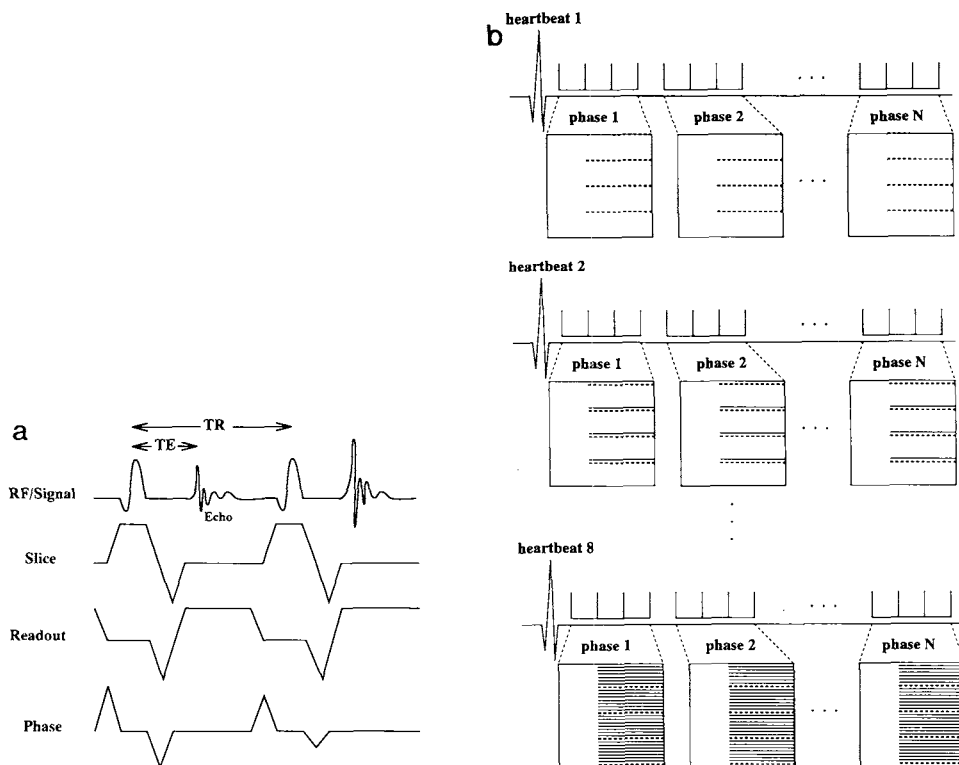


FIG. 2. (a) Two echoes from the GRASS pulse sequence used to obtain the cine images. All gradient waveforms use maximum slew rate ramps. The slice selection gradient has maximum amplitude. A “fractional echo” is used to sample in the readout direction. The phase encoding “rewinder” gradient overlaps with the ascending ramp of the slice selection gradient for the next acquisition. (b) The segmented  $k$ -space mapping used to obtain the tagged cine images. In the acquisition shown, four lines of  $k$ -space are sampled in each movie phase (dashed lines),  $N$  total movie phases are acquired, and eight heartbeats are used to acquire the data matrix. For this example a final data matrix of  $32 \times 160$  is obtained for each movie phase. More phase encoding steps can be achieved by using more heartbeats or using more views per movie phase. Note: the  $k$ -space map is not to scale.

encoding pulses used during eight heartbeats to produce an  $N$  phase movie of the cardiac cycle. Each movie phase has the same four lines of  $k$ -space filled consecutively in each heartbeat. The order in which the  $k_y$  lines of  $k$ -space are filled is adjustable to minimize ghost artifacts. The number of heartbeats, the number of  $k$ -space lines per heartbeat, and the number of movie phases are all adjustable. These values are determined by patients' ability to hold their breath, the required insensitivity to motion blurring, and the required time resolution.

The tagging sequence was triggered by the upslope of the QRS from the ECG; the imaging acquisition occurred immediately following the tagging. A parallel line tagging pattern was produced with the pulse sequence shown in Fig. 3a. This is a hybrid DANTE/SPAMM sequence (2, 9) of seven pulses with the dispersion gradient reduced for the application of each pulse. The amplitude of the gradient during the application

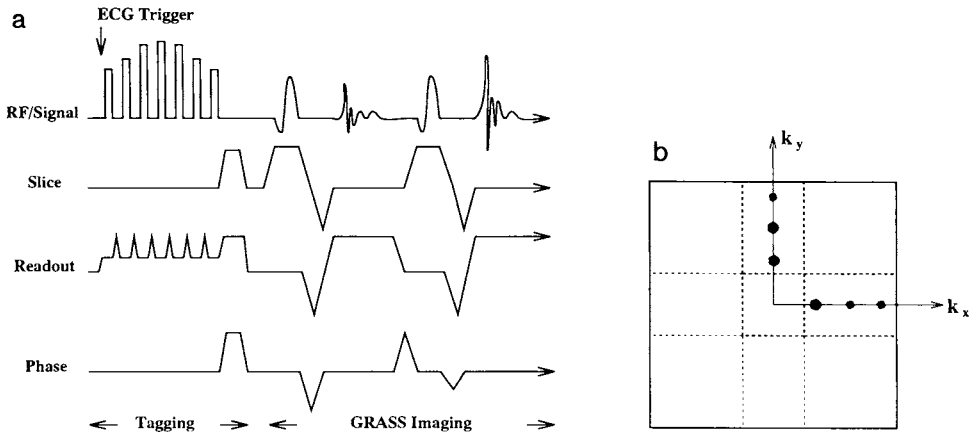


FIG. 3. (a) The hybrid DANTE/SPAMM tagging pulse sequence. The parallel line tagging pattern is produced by a sequence of rectangular pulses. The gradient producing the dispersion in the sample is reduced during the rf pulses to reduce the total bandwidth required from the pulse to tag the heart. This permits the use of longer lower amplitude rectangular pulses. The tagging pulses are triggered by the upslope of the QRS complex and the imaging pulses follow immediately after spoiler gradients dephase transverse magnetization from the tagging pulses. (b) The “cross” pattern used to sample  $k$ -space for the final grid-tagged images. The Fourier components of the tagging pattern (schematically shown as black dots) are limited to the regions around the axes. The regions sampled with the pulse sequence are enclosed by the bold dashed lines; the regions obtained through symmetry are in the light dashed lines.

of the hard pulses can be adjusted so that the bandwidth of the region in the patient to be tagged is matched with the bandwidth of the rf pulse. The advantages of this parallel line tagging sequence are discussed under Conclusion and Discussion.

#### *Data Acquisition Protocol*

The volunteer was instructed to hold his/her breath at end-expiration to minimize registration errors. The volunteer was placed prone on the quadrature T/L surface coil (GE Medical Systems, Milwaukee, WI). ECG leads were placed on the volunteer's back and the upslope of the QRS complex was used to trigger the acquisition. A set of eight coronal scout scans were obtained in two 16-heartbeat breath-holds using the pulse sequence shown in Fig. 2 in single phase mode. The imaging parameters were field-of-view = 34 cm, TR = 5.8 ms, TE = 2.1 ms,  $\alpha = 20^\circ$ , number of phase encode views per heartbeat = 16,  $64 \times 160$  sampling matrix, voxel size  $1.5 \times 3.0 \times 10$  mm, one excitation. From these images, graphic prescription was used to define a stack of single oblique views of the heart, approximating a short axis orientation. These images were obtained with the same parameters as the previous series. The centroid of the left ventricle at the base and the apex as measured from these single oblique scout images was then used to explicitly prescribe the stack of short axis images. The total imaging time used to obtain the prescription of the stack of short axis images was 32 heartbeats in four breath-holds.

A tagged cine sequence for each short axis section was obtained with the pulse sequence shown in Fig. 3a. Six 10-mm contiguous slices were obtained. For each slice,

two cine sequences were obtained in a single breath-hold. In the first 8 heartbeats a set of parallel tags was oriented perpendicular to the readout direction; in the second 8 heartbeats the direction of the readout and phase gradients was swapped and an orthogonal set of parallel tags was used. This protocol gives high-resolution sampling of the parallel tags in two orthogonal directions by using the “cross” sampling of  $k$ -space shown in Fig. 3b. Performing both orientations in a single breath-hold ensures that there is no misregistration for the slice. A set of long axis images was then graphically prescribed from the short axis images with a radial orientation (5). A cine sequence for each long axis section was obtained with the same protocol that was used for the short axis images. In each case the tags were oriented parallel to the short axis planes and the readout gradients were oriented perpendicular to the tags. The total image acquisition time for the 3D strain data was 144 heartbeats in 12 breath-holds. Each breath-hold was 16 heartbeats, or about 14 s.

## RESULTS

### *Breath-Hold Tagged Images*

A sequence of 6 phases from an 8-phase cine acquisition of a short axis slice is shown in Fig. 4. The parameters for this acquisition were TR = 5.9 ms, TE = 2.3 ms,  $\alpha = 20^\circ$ , one excitation, the number of phase encode views per heartbeat was 8, the total number of heartbeats was 16. Two orientations of the parallel tagging pattern are shown; the data for both orientations were obtained in the same breath-hold. In each case, the readout direction is perpendicular to the tags. Figure 5 shows a sequence of 6 phases from an 8-phase cine acquisition of a long axis slice. The imaging parameters were the same as those used for the short axis views. Only one orientation of the tags is necessary for tracking motion of the heart wall in the direction perpendicular to the short axis images. The total number of cine phases achievable is limited by the speed of the microprocessor controlling the sequence. If TR is lengthened to 6.4 ms, 32 cine phases may be used.

### *Grid Tagged Images*

In order to display the two-dimensional strain field in the short axis planes the two orthogonal tagged images are combined with the operation

$$s_{\text{grid}}(i, j) = \min \{ s_{\text{vert}}(i, j), s_{\text{horiz}}(i, j) \}, \quad [1]$$

where  $s_{\text{grid}}(i, j)$  is the grid image and  $s_{\text{vert}}(i, j)$   $s_{\text{horiz}}(i, j)$  are the individual parallel tag images for the slice at a given time. This operation retains the tags from both the horizontal and vertical orientations. Figure 6 shows 6 movie phases of grid images created in this way.

### *Effect of $k$ -Space Sampling*

Because the Fourier coefficients of the  $x = \text{constant}$  parallel line pattern are limited to the region of  $k$ -space around the  $k_y = 0$  line, it is possible to reduce the phase encode views dramatically without severely reducing the ability to resolve the parallel lines. We were able to resolve the parallel lines from images obtained using as few as

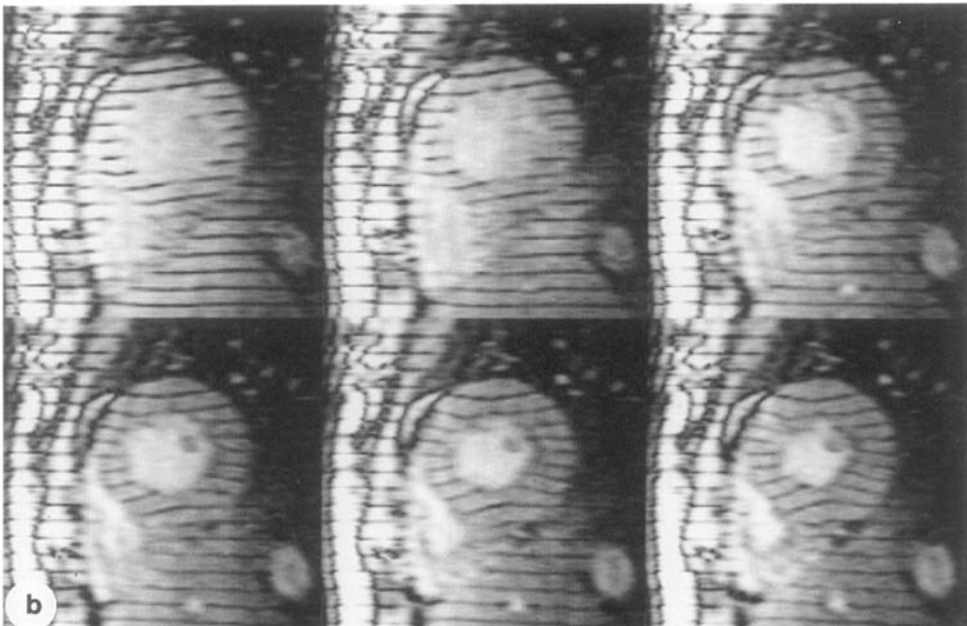
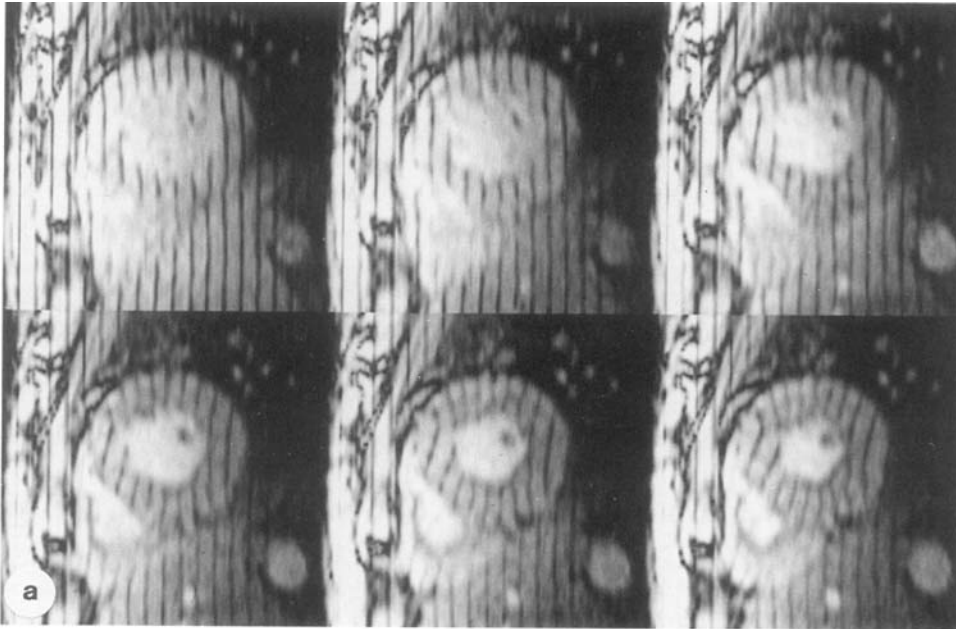


FIG. 4. Six phases of the cardiac cycle as imaged in the short axis orientation with the tagged cine protocol. The images were obtained with a time resolution of 48 ms. (a) The readout gradient is oriented in the horizontal direction with the parallel tags in the vertical direction. (b) The readout gradient is oriented in the vertical direction with the parallel tags in the horizontal direction.

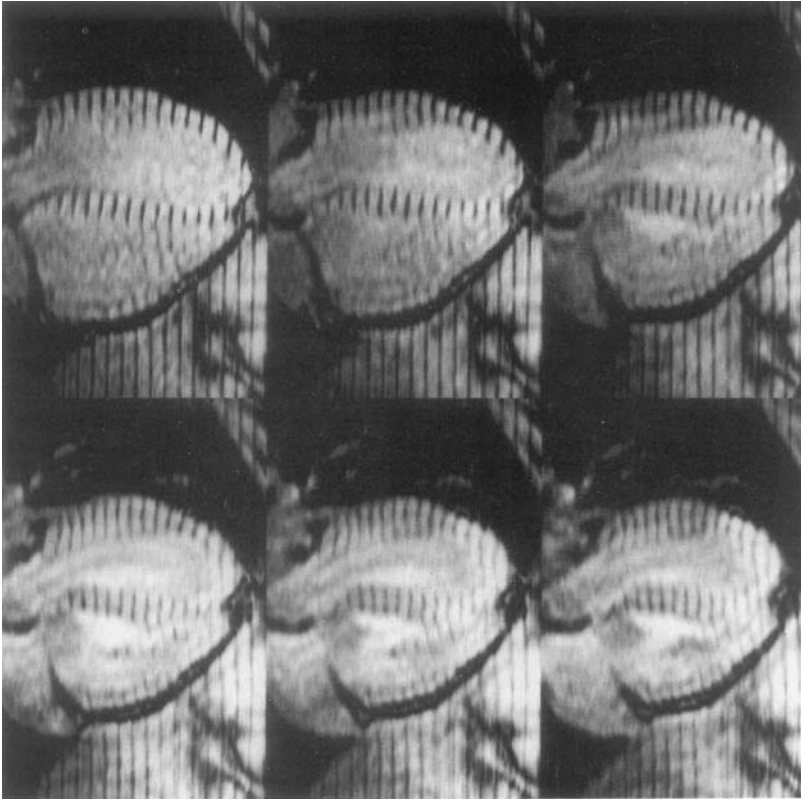


FIG. 5. Six phases of the cardiac cycle as imaged in the long axis orientation with the tagged cine protocol. The tags are oriented in parallel planes with the short axis images; the readout gradient is oriented perpendicular to the tags. These images are important for 3D tracking of tissue through the short axis imaging planes.

32 phase encoding steps and a rectangular field-of-view. Figure 7a shows 4 phases from an 8-phase movie obtained in four heartbeats. The number of phase encode views (NPE) was 32 and the number of phase encode views per movie phase (NVP) was 8 which gives a time resolution of 48 ms. The images in Fig. 7b were acquired with the same parameters except NVP was set to 4. In this case, the data were acquired over eight heartbeats and the movie phases were separated by 24 ms. While the signal-to-noise ratio is not good in these images, the four-heartbeat acquisition has remarkably well-resolved tag lines.

#### CONCLUSION AND DISCUSSION

We have developed an imaging sequence to obtain tagged cardiac cine studies in a breath-hold. The TR value obtained for the GRASS pulse sequence used to acquire the data is as short as 5.8 ms for a 24-cm field-of-view. This allows us to scan multiple lines of  $k$ -space in each heartbeat while maintaining good time resolution in the cine phases. Motion sensitivity is reduced by using a short TE; for nonoblique planes the

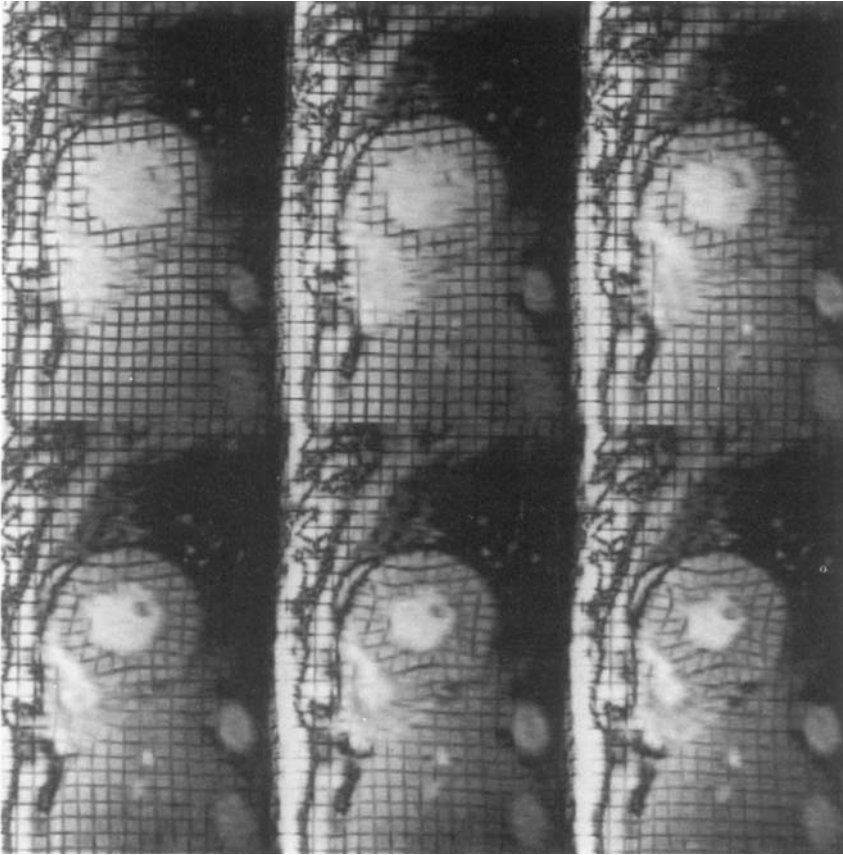


FIG. 6. Six phases of the heart cycle with a grid tag pattern derived using Eq. [1] and the parallel tag images shown in Fig. 4.

sequence has a 2.1-ms TE for a 24-cm field-of-view. The minimum achievable TR and TE values are functions of field-of-view, the orientation of the scanning plane and the fraction of  $k$ -space covered by the readout gradient.

A parallel line sequence was used instead of a grid for a number of reasons. It takes one-half of the time to produce the tagging pattern which reduces the sensitivity to motion. The Fourier coefficients of the parallel line pattern are close to a single line of  $k$ -space for all times; this allows reduction in the number of phase encode views without losing precision in estimating the position of the tag lines. Automated quantitative analysis on the images with the parallel pattern is simple to perform. The signal intensity of the parallel tagging lines is easier to model. There is no interference between the magnetization of orthogonal tagging planes allowing us to pack the lines closer together. The signal-to-noise ratio of the images is higher with the parallel lines letting us sample farther out into the cardiac cycle. For visual display, the grid images are easily constructed from images with orthogonal parallel tag lines. This image cor-

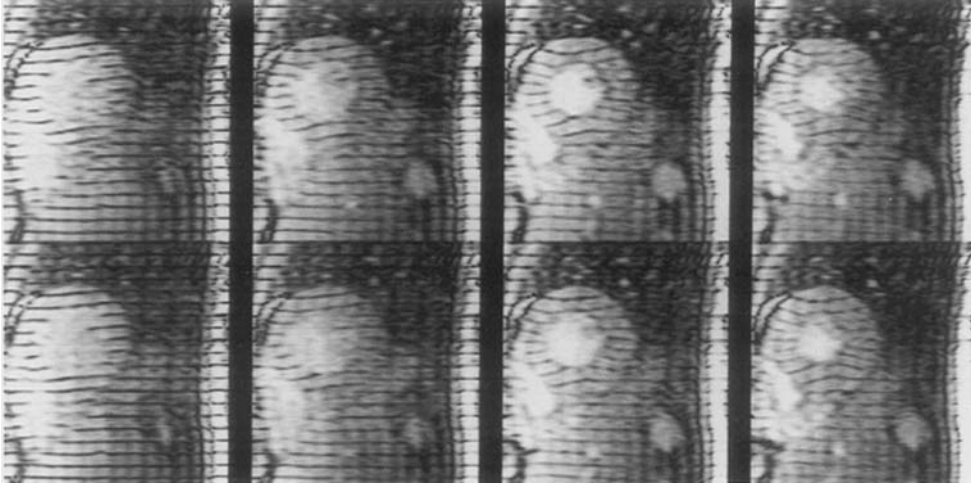


FIG. 7. The effect of reduced phase encoding resolution and  $k$ -space segmentation. The acquisition parameters were field-of-view = 28 cm, TR = 6.0 ms, TE = 2.3 ms,  $\alpha = 20^\circ$ , 1 NEX, and rectangular field-of-view. (Top) A four-heartbeat acquisition. The number of phase encode views (NPE) is 32, and number of phase encode views per movie phase (NVP) is 8, 48 ms time resolution in the movie phases. (Bottom) An eight-heartbeat acquisition, NPE = 32, NVP = 4, 24 ms time resolution in the movie phases.

responds to a “cross” sampling of  $k$ -space; performing the combination in the spatial domain avoids artifacts from phase discontinuities in the raw data.

In order to minimize the time needed to produce the tagging pattern we modified the DANTE sequence by reducing the gradient amplitude during the rf pulse as shown in Fig. 3a. Setting the gradient amplitude during the rf pulse to zero gives a one-dimensional SPAMM sequence (2) and the entire image is tagged. However, the spacing of the tags is determined by the integral of the gradient between the pulses and the sharpness of the tag profile is determined by the total number of rf pulses. It is advantageous to maximize the number of rf pulses in the tagging train because the precision of estimating the tag position and the maximum density of the tag lines in the tissue will increase with the number of rf pulses used (6). The duration of the tagging sequence can be minimized for a given tag spacing and total number of pulses by setting the gradient to a nonzero value during the rf pulses.

While tagging can be performed in a single heartbeat with echo-planar imaging (10), gradient-recalled acquisition has some advantages over echo-planar imaging of the heart: arbitrary oblique imaging planes are easily achieved, standard scanner hardware can be used, short encoding times virtually eliminate artifacts from the buildup of flow-induced phase shifts, and a large number of cine phases can be obtained in a relatively low number of heartbeats. It is clear that the images with 64 phase encoding steps and 8 phase encoding steps per cine frame shown in Fig. 4 produce images that are adequate for measuring the two-dimensional strain field. For normal volunteers a 32-heartbeat breath-hold is possible; for patients, an 8- to 16-heartbeat breath-hold is used routinely; from Fig. 7a, a 4-heartbeat acquisition, while not ideal, seems also possible.

The acquisition parameters demonstrated in this paper were determined by hardware limitations or by experiment. We must still optimize many parameters for these data acquisitions quantitatively: the type of pulse sequence, TE and receiver bandwidth, TR, flip angle, rf pulse duration and slice selection gradient amplitude, tag spacing, tag flip angle, number and order of the phase encoding steps, and number of  $k$ -space lines per cine phase per heartbeat. Also, methods for automated analysis that include detection and correction of registration errors from different breath-holds must be developed. This work will be reported in a subsequent publication.

The impact of this sequence on cardiac tagging studies will be significant. The total time for a 3D volume exam is now on the order of 15 min, whereas with the multislice, multiphase spin-echo acquisitions the examination time was between 60 and 90 min. The sensitivity of the technique to irregular heartbeats is low because so few heartbeats are required for each cine sequence. The limiting factor for the further reduction of the examination time is the speed of the technologist, image reconstruction time, and the response time of the computer associated with the scanner. With the addition of a specialized coil to increase the signal-to-noise of the myocardial signal, 3D motion measurements in the human heart may be possible in as few as three breath-holds.

#### ACKNOWLEDGMENTS

This research was supported by the National Institutes of Health Grants R29-HL45683 and R01-HL45090. E. R. McVeigh is a recipient of a Radiological Society of North America Scholar award. Ergin Atalar is partially supported through a Whitaker postdoctoral fellowship and a grant from Bilkent University. The authors thank Michael Guttman, Steve Einstein, and Elias Zerhouni for their help with this work. We also thank Anna Holsinger and Steve Riederer for suggesting "board-looping" on the Signa.

#### REFERENCES

1. E. A. ZERHOUNI, D. M. PARISH, W. J. ROGERS, A. YANG, AND E. P. SHAPIRO, *Radiology* **169**, 59 (1988).
2. L. AXEL AND L. DOUGHERTY, *Radiology* **171**, 841 (1989).
3. N. J. PELC, R. J. HERFKENS, AND ENZMAN D. R. SHIMIKAWA, *Magn. Reson. Q.* **7**(4), 229 (1991).
4. E. R. MCVEIGH AND E. A. ZERHOUNI, *Radiology* **180**, 677 (1991).
5. C. C. MOORE, W. G. O'DELL, E. R. MCVEIGH, AND E. A. ZERHOUNI, *J. Magn. Reson. Imaging* **2**, 165 (1992).
6. E. ATALAR AND E. R. MCVEIGH, In "Eleventh Annual Meeting of SMRM, Book of Abstracts, 1992," p. 4225.
7. D. J. ATKINSON AND R. R. EDELMAN, *Radiology* **178**, 357 (1991).
8. A. P. CRAWLEY, M. L. WOOD, AND R. M. HENKELMAN, *Magn. Reson. Med.* **8**, 248 (1988).
9. T. J. MOSHER AND M. B. SMITH, *J. Magn. Reson.* **15**, 334 (1990).
10. S. J. BLACKBAND, J. C. CHATHAM, J. FORDER, AND E. R. MCVEIGH, In "Tenth Annual Meeting of SMRM, Book of Abstracts, 1991," p. 256.